CONFIDENTIAL

Copy 5
RM H57D17a

NACA RM H57D17a

UNCLASSIFIED

NACA

RESEARCH MEMORANDUM

AIRPLANE MOTIONS AND LOADS INDUCED BY FLYING THROUGH THE FLOW FIELD GENERATED BY AN AIRPLANE AT LOW SUPERSONIC SPEEDS

By Gareth H. Jordan, Earl R. Keener, and Stanley P. Butchart

High-Speed Flight Station
Edwards, Calif.

NATIONAL ADVISORY COMMITTEE FOR AERONAUTICS

WASHINGTON

June 7, 1957

CONFIDENTIAL

[redacted]

NATIONAL ADVISORY COMMITTEE FOR AERONAUTICS

RESEARCH MEMORANDUM

AIRPLANE MOTIONS AND LOADS INDUCED BY FLYING THROUGH THE FLOW FIELD GENERATED BY AN AIRPLANE AT LOW SUPERSONIC SPEEDS

By Gareth H. Jordan, Earl R. Keener,
and Stanley P. Butchart

SUMMARY

An exploratory flight investigation was conducted to determine the disturbances to an airplane while flying in formation with another airplane at low supersonic speeds. The most significant motions were encountered as a result of flying through the flow field of the lead airplane. Several of these supersonic passes were made using two swept-wing fighter-type airplanes in order to evaluate the gross effects of time to pass through the flow field, lateral distance, and altitude within a Mach number range from 1.1 to 1.3.

Significant airplane motions and vertical-tail loads can be experienced as a result of close-proximity side-by-side passes at supersonic speed. The most severe motions and vertical-tail loads were experienced during passes made at separation distances less than 100 feet and at a time to pass near and slightly greater than the airplane natural period in yaw. The passing airplane experienced maximum sideslip angles of about 5.4° and maximum vertical-tail loads of approximately 50 percent of design limit in shear, bending moment, and torsion. Maximum vertical-tail loads can be determined essentially from the maximum airplane sideslip angle and the vertical-tail lift-curve slope. Increasing the lateral separation distance was shown to decrease the maximum sideslip angle and, thus, to reduce the maximum vertical-tail load.

INTRODUCTION

Military pilots have reported that severe disturbances are encountered while flying in formation at supersonic speed. The implication of these reports was that severe loading conditions might be imposed on an airplane by flying in the flow field generated by another airplane at supersonic speed. As a result of these reports, the NACA High-Speed Flight Station at Edwards, Calif., has conducted an exploratory flight investigation to

[redacted]

determine the nature and severity of the disturbances that might be encountered. During the investigation, it was found that the most significant airplane motions and loads were imposed on the airplane as a result of flying through the flow field in a passing maneuver.

The purpose of this paper is to summarize the results of this investigation and to point out some of the factors believed to be important in an assessment of the overall problem of supersonic passes. The experimental data were obtained at Mach numbers from 1.1 to 1.3 at altitudes from 20,000 to 40,000 feet.

SYMBOLS

c	chord, ft (fig. 1)
F_a	aileron stick force, lb
F_r	rudder pedal force, lb
F_s	stabilizer stick force, lb
$F_{Y,v}$	vertical-tail structural load, lb
g	acceleration due to gravity, ft/sec^2
h_p	pressure altitude, ft
I_X	moment of inertia about X-axis, slug-ft^2
I_Y	moment of inertia about Y-axis, slug-ft^2
I_Z	moment of inertia about Z-axis, slug-ft^2
I_{XZ}	product of inertia, slug-ft^2
i_t	incidence angle of all-movable stabilizer, positive when leading edge up, deg
M	Mach number as measured by airspeed head mounted on nose boom
$M_{b,v}$	vertical-tail structural bending moment, in-lb
n_Y	transverse-load factor, g units

n_Z	normal-load factor, g units
P_n	period of natural frequency of airplane in yaw, sec
p	static pressure as measured by airspeed head mounted on nose boom, lb/sq ft, or rolling angular velocity, radians/sec
Δp	approximate variation of static pressure in flow field from free stream
$\dot{p}$	rolling angular acceleration, radians/sec^2
q	free-stream dynamic pressure, lb/sq ft, or pitching angular velocity, radians/sec
$\dot{q}$	pitching angular acceleration, radians/sec^2
r	yawing angular velocity, radians/sec
$\dot{r}$	yawing angular acceleration, radians/sec^2
T_V	vertical-tail structural torque, in-lb
t	time, sec
y	lateral separation distance between flight paths of airplanes, ft
α	airplane angle of attack as measured at nose boom, deg
β	airplane angle of sideslip as measured at nose boom, deg
δ_a	total aileron deflection, deg
δ_r	rudder deflection, deg
ζ	damping ratio

Subscript:

max	maximum

DESCRIPTION OF AIRPLANE AND INSTRUMENTATION

The test airplane used for this investigation was a swept-wing fighter-type airplane capable of supersonic speed in level flight. A three-view drawing of the airplane giving overall dimensions is presented in figure 1. The physical characteristics are given in table I.

The test airplane used for these studies was instrumented to measure quantities pertinent to these investigations. Structural loads on the test airplane were measured by strain gages located at the root of each surface. The strain-gage station and torque axis for the vertical-tail loads are shown in figure 1.

The airspeed head from which static-pressure measurements were obtained and the angle-of-sideslip vane were mounted on the nose boom of the test airplane. Pertinent dimensions of this installation are shown in figure 2.

The lead airplane for these formation flights was furnished by the Air Force Flight Test Center and was an uninstrumented airplane of the same type as the test airplane.

TESTS

The motions and loads associated with supersonic passes were investigated by the test procedure shown in figure 3. The instrumented test airplane was flown through the flow field generated by the lead airplane in a side-by-side passing maneuver. These supersonic passes were made at various lateral separation distances and at various passing rates within a Mach number range of 1.1 to 1.3 and at altitudes from 20,000 to 40,000 feet. The speed differentials for the passing rates investigated varied from about 5 feet per second to 50 feet per second or incremental Mach numbers less than 0.05.

RESULTS AND DISCUSSION

Factors Involved

Some of the factors that should be considered in a general assessment of the supersonic pass problem are as follows:

Mach number
altitude

rate of passing
separation distance

relative flight paths

relative size
initial conditions
stability
configuration

The dynamic pressure, which has a direct bearing on the loads, is determined by Mach number and altitude. Mach number and altitude also determine the physical characteristics of the flow field and the strength of the shocks in the flow field for a given configuration. The effect of rate of passing and lateral separation distance on the response of the airplane to the flow-field disturbance is discussed in the presentation of the experimental results to follow. Only the side-by-side pass has been investigated; however, many variations in relative flight paths are possible, such as overhead passes, head-on passes, and curved flight paths. No experimental results are available to indicate the effect of relative size of the lead and passing airplanes, initial conditions before passing, stability, or configuration; however, these factors must be considered before a complete assessment of the problem can be made. It should be pointed out that, although this investigation concerns the motions and loads experienced by the passing airplane, a similar disturbance was felt by the other airplane as the flow field of the passing airplane swept over it.

Time History of a Supersonic Pass

In order to have a more complete understanding of the supersonic pass problem and of the resulting airplane motions and loads, a more detailed sketch of the flow field and a time history of a supersonic pass are shown in figures 4 and 5. The flight conditions for this supersonic pass are $M \approx 1.3$, $h_p \approx 32{,}400$ feet, $y \approx 100$ feet, and a speed differential of about 12 feet per second. In figure 4, the lead airplane and a portion of the shocks generated by this airplane are shown. For simplicity, the shocks are represented by parallel lines at the Mach angle for $M = 1.3$. The flow field is further assumed to be one fuselage length in a direction parallel to the flight path. The incremental pressure changes within the flow field were obtained from the airspeed record during this supersonic pass and are shown in the lower part of the figure. The three stronger shocks resulted in abrupt pressure jumps of 15 to 17 pounds per square foot. In addition, the approximate path of a streamline (somewhat exaggerated) through this flow field is indicated in figure 4 and the test airplane is shown just entering the flow field. From a consideration of the flow direction, it may be seen that the test airplane experiences a local lateral velocity over its fuselage and then over its tail as the flow field is traversed; hence, the test airplane experiences a yawing-moment input.

From the time histories of the measured quantities in figure 5, it is seen that the test airplane experienced an excursion in sideslip in which a maximum sideslip angle of 4.7° was measured. The maximum lateral acceleration associated with this airplane motion was $\pm 0.7g$. The vertical-tail loads in figure 5(c) are mainly a function of the airplane sideslip angle; and the maximum vertical-tail shear, bending moment, and torque measured during this pass were about 50 percent of design limit.

Maximum Sideslip Angle

A summary of the supersonic passes performed within a Mach number range of 1.1 to 1.3 at altitudes from 20,000 feet to 40,000 feet is shown in figure 6. The maximum sideslip angles measured during these passes are shown as a function of time to pass. Time to pass is defined as the time in seconds required for any part of the test airplane to traverse the distance from the trailing shock to the bow wave of the generating airplane and was determined for these tests from the airspeed-head static-pressure record. The time-to-pass values in figure 6 represent speed differentials from about 50 feet per second at the fast rate of passing to about 5 feet per second at the slow rate of passing. Also shown in this figure is the natural period of the airplane in yaw for the range of Mach number and altitude of these passes.

The solid symbols in figure 6 represent the maximum sideslip response measured during passes made at separation distances less than 100 feet, the half-solid symbols represent passes at distances from 100 feet to 300 feet, and the open symbols represent passes made at distances greater than 400 feet. The effect of distance may be seen by comparing the response of the airplane at various distances. As would be expected, the largest response was obtained at distances less than 100 feet and the response is seen to decrease as the separation distance is increased.

A noticeable effect of rate of passing may be seen by comparing the response of the airplane at distances less than 100 feet. For a time to pass considerably less than the natural period of the airplane in yaw, very little airplane motion was encountered. At times to pass near and greater than the natural period, significant airplane sideslip angles were obtained. In addition, a small reduction in sideslip response is evident at the higher time-to-pass values.

The effect of Mach number on the airplane motions could not be determined because of the limited range of Mach number investigated. No effect of altitude on the airplane motion was found within the range investigated (20,000 to 40,000 feet).

It is apparent from these data that there is some dynamic response to the flow-field disturbance. Some preliminary calculations were made in an effort to predict the maximum airplane motions. These calculations were based on the simple dynamic response of a linear single-degree-of-freedom system to a yawing-moment input. (See, for example, ref. 1.) The results of these calculations are compared with the flight results in figure 7. The data in this figure have been corrected to a lateral separation distance of 100 feet by the expression $\beta_{max}\sqrt{y/100}$. This correction is based on some theoretical work by G. B. Whitham (ref. 2) in which it is shown that the lateral velocity in the flow field of a body at supersonic speed varies inversely with the square root of the lateral separation distance. The curve of the calculated response is based on a damping ratio of 0.07 which corresponds to the flight-determined damping ratio of the airplane at low supersonic Mach numbers (ref. 3). These calculations predict extremely large sideslip angles near the airplane natural period that have not been realized in flight. It is evident that more refined calculations are necessary before reliable estimates of the maximum airplane motions can be predicted. Additional calculations employing an analysis based on the recent traveling-gust concept are presently under way.

Maximum Vertical-Tail Loads

A summary of the maximum vertical-tail loads (measured during these supersonic passes) is shown in figure 8. The maximum vertical-tail loads have been corrected to an altitude of 30,000 feet by a dynamic-pressure correction. On the left-hand side of the figure, the maximum vertical-tail loads measured during passes at distances less than 100 feet are shown as a function of time to pass. The vertical-tail loads vary in a manner similar to that previously shown for maximum sideslip angle, and vertical-tail loads of 50 percent of design limit were experienced at a time-to-pass slightly greater than the natural period of the airplane in yaw.

As a matter of interest, the fast rate of passing resulted in negligible airplane motion and, thus, in relatively small vertical-tail loads. Some evidence of structural excitation was visible, however, in the flight records for this pass. This excitation is a result of an impact type of loading imposed on the vertical tail during high passing rates.

On the right-hand side of figure 8 the maximum vertical-tail loads from all of the supersonic passes are shown as a function of the maximum sideslip angle. Also included is the variation of the vertical-tail load based on the experimental lift-curve slope of the vertical tail from other experimental results. A comparison of the vertical-tail loads experienced during these passes with the experimental lift-curve slope indicates that the maximum vertical-tail loads can be determined from the maximum airplane sideslip angle and the vertical-tail lift-curve slope.

As previously mentioned the magnitude of the airplane motions was found to be relatively unaffected by altitude within the range of this investigation. It might be expected that loads in excess of design limit would be experienced as a result of close-proximity passes at an altitude lower than the range investigated because of the increase in dynamic pressure.

Pilot's Comments

Formation flying at supersonic speeds does not differ from subsonic formation work as long as the wingman remains in a position behind the flow field of the lead airplane. If the wingman gets out of position, either by overshooting during join up or by drawing abreast of the lead plane as a result of a turn-in maneuver of the lead plane, control of the airplane can become quite difficult.

If the wingman moves ahead slowly, the first encounter with the flow field of the lead airplane causes an abrupt yaw toward the lead plane. (The first impression is that you will fly right through the middle of the lead airplane.) A little difficulty is experienced in holding vertical position at this point also, not unlike flying in the wing wake of another airplane at slower speeds. It is possible to retrim and to hold formation position after the airplane has penetrated some distance into the flow field. Moving ahead a little farther releases the yaw toward the lead plane and sets up a slight yaw in the opposite direction. It is possible to move out from the lead airplane for a distance of 500 to 600 feet or more and still remain in this yawed position.

The most startling experience occurs when the wingman slides up past the lead aircraft at a speed where the yaw toward the lead plane and then away from the lead plane comes in phase with the natural frequency of the airplane in yaw. Under this condition the airplane ends up in a yawing oscillation that can be four or five times greater than that attainable when rudder alone is used at that same speed. The airplane controls are not effective in preventing the oscillation and the airplane feels out of control for a few seconds.

CONCLUDING REMARKS

Results of an investigation of airplane motions and loads induced by flying through the flow field of an airplane at low supersonic speeds have indicated that significant airplane motions and vertical-tail loads can be experienced as a result of close-proximity side-by-side passes at supersonic speed. The most severe motions and vertical-tail loads were experienced during passes made at separation distances less than 100 feet and at a time to pass near and slightly greater than the airplane natural period in yaw. The passing airplane experienced maximum sideslip angles of about 5.4° and maximum vertical-tail loads of approximately 50 percent of design limit in shear, bending moment, and torsion. Maximum vertical-tail loads can be determined essentially from the maximum airplane sideslip angle and the vertical-tail lift-curve slope. Increasing the lateral separation distance was shown to decrease the maximum sideslip angle and, thus, to reduce the maximum vertical-tail load.

A general assessment of the problem of supersonic passes requires that several additional factors be considered - namely, effects of Mach number, stability, configuration, relative size, and relative flight path on the airplane motions and loads.

High-Speed Flight Station,
National Advisory Committee for Aeronautics,
Edwards, Calif., March 5, 1957.

REFERENCES

1. Triplett, William C., Brown, Stuart C., and Smith, G. Allan: The Dynamic-Response Characteristics of a 35° Swept-Wing Airplane As Determined From Flight Measurements. NACA Rep. 1250, 1955. (Supersedes NACA RM A51G27 by Triplett and Smith and RM A52I17 by Triplett and Brown.)

2. Whitham, G. B.: The Flow Pattern of a Supersonic Projectile. Communications on Pure and Appl. Math., vol. V, no. 3, Aug. 1952, pp. 301-348.

3. Wolowicz, Chester H.: Time-Vector Determined Lateral Derivatives of a Swept-Wing Fighter-Type Airplane With Three Different Vertical Tails at Mach Numbers Between 0.70 and 1.48. NACA RM H56C20, 1956.

TABLE I

PHYSICAL CHARACTERISTICS OF THE TEST AIRPLANE

Wing:	
Airfoil section	NACA $64_{(06)}$A007
Total area (including aileron and 83.84 sq ft covered by fuselage), sq ft	385.21
Span, ft	38.58
Mean aerodynamic chord, ft	11.16
Root chord, ft	15.86
Tip chord, ft	4.15
Taper ratio	0.262
Aspect ratio	3.86
Sweep at 25-percent-chord line, deg	45
Incidence, deg	0
Dihedral, deg	0
Geometric twist, deg	0
Aileron:	
Area rearward of hinge line (each), sq ft	19.32
Span at hinge line (each), ft	7.81
Chord rearward of hinge line, percent wing chord	25
Travel (each), deg	±15
Leading-edge slat:	
Span, equivalent, ft	12.71
Segments	5
Spanwise location, inboard end, percent wing semispan	23.3
Spanwise location, outboard end, percent wing semispan	89.2
Ratio of slat chord to wing chord (parallel to fuselage reference line), percent	20
Rotation, maximum, deg	15
Horizontal tail:	
Airfoil section	NACA 65A003.5
Total area (including 31.65 sq ft covered by fuselage), sq ft	98.86
Span, ft	18.72
Mean aerodynamic chord, ft	5.83
Root chord, ft	8.14
Tip chord, ft	2.46
Taper ratio	0.30
Aspect ratio	3.54
Sweep at 25-percent-chord line, deg	45
Dihedral, deg	0
Travel, leading edge up, deg	5
Travel, leading edge down, deg	25

TABLE I.- Continued

PHYSICAL CHARACTERISTICS OF THE TEST AIRPLANE

Vertical tail:	
Airfoil section	NACA 65A003.5
Area (excluding dorsal fin and area blanketed by fuselage), sq ft	42.7
Area blanketed by fuselage (area between fuselage contour line and line parallel to fuselage reference line through intersections of leading edge of vertical tail and fuselage contour line)	2.45
Span (unblanketed), ft	7.93
Mean aerodynamic chord, ft	5.90
Root chord, ft	8.28
Tip chord, ft	2.49
Taper ratio	0.301
Aspect ratio	1.49
Sweep at 25-percent-chord line, deg	45
Rudder:	
Area, rearward of hinge line, sq ft	6.3
Span at hinge line, ft	3.33
Root chord, ft	2.27
Tip chord, ft	1.50
Travel, deg	±20
Spanwise location, inboard end, percent vertical-tail span	3.1
Spanwise location, outboard end, percent vertical-tail span	44.8
Chord, percent vertical-tail chord	28.4
Aerodynamic balance	Overhanging, unsealed
Fuselage:	
Length (afterburner nozzle closed), ft	45.64
Maximum width, ft	5.58
Maximum depth over canopy, ft	6.37
Side area (total), sq ft	230.92
Fineness ratio (afterburner nozzle closed)	7.86
Speed brake:	
Surface area, sq ft	14.14
Maximum deflection, deg	50
Powerplant:	
Turbojet engine	One Pratt & Whitney J57-P7 with afterburner
Thrust (guarantee sea level), afterburner, lb	15,000
Military, lb	9,220
Normal, lb	8,000

TABLE I.- Concluded

PHYSICAL CHARACTERISTICS OF THE TEST AIRPLANE

Airplane weight, lb:	
Basic (without fuel, oil, water, pilot)	19,662
Total (full fuel, oil, water, pilot)	24,800
Center-of-gravity location, percent mean aerodynamic chord:	
Total weight - gear down	31.80
Total weight - gear up	31.80
Moments of inertia (estimated total weight):	
I_X, slug-ft^2	11,103
I_Y, slug-ft^2	59,248
I_Z, slug-ft^2	67,279
I_{XZ}, slug-ft^2	941
Inclination of principal axis (estimated total weight):	
Below reference axis at nose, deg	0.8

TEST AIRPLANE

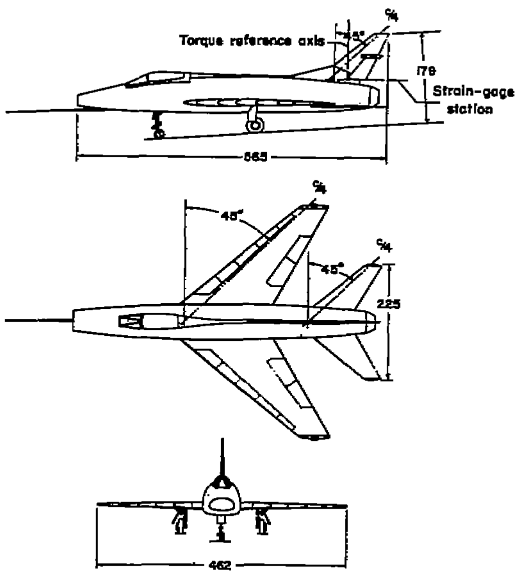

Figure 1

INSTRUMENTATION ON NOSE BOOM OF TEST AIRPLANE

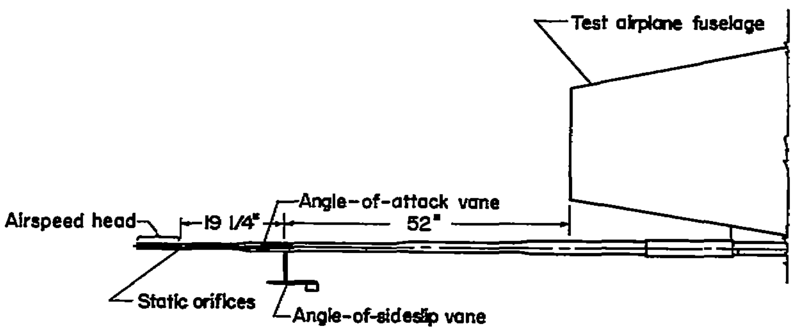

Figure 2

DESCRIPTION OF TESTS

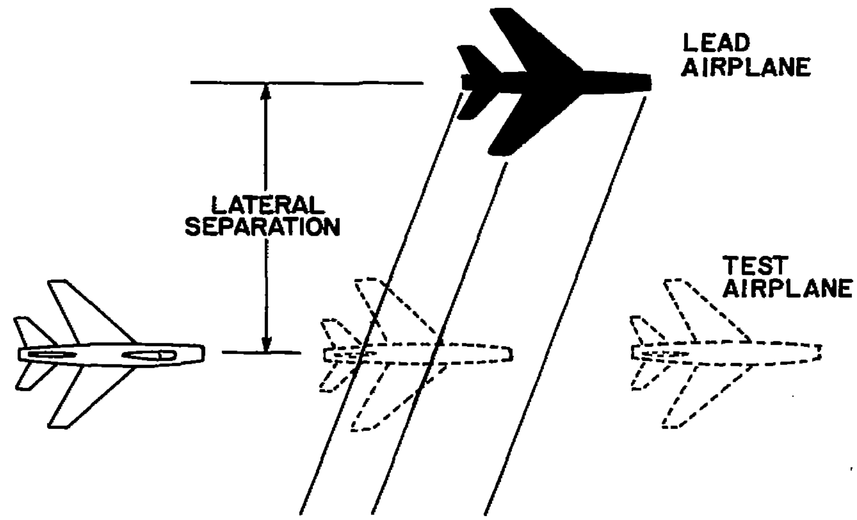

Figure 3

SKETCH OF SIMPLIFIED FLOW FIELD

$M \approx 1.3$; $h_p \approx 32{,}400$ FEET

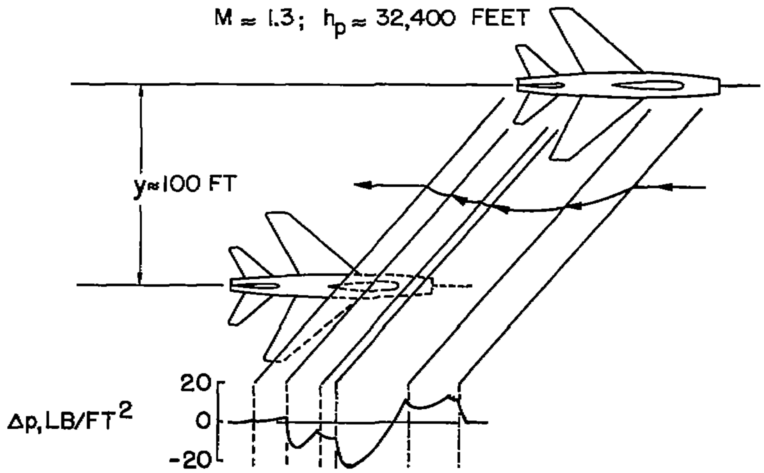

Figure 4

TIME HISTORY OF SUPERSONIC PASS; M≈1.3; h_p≈32,400; y≈100

AIRPLANE ANGULAR MOTIONS AND LOAD FACTORS

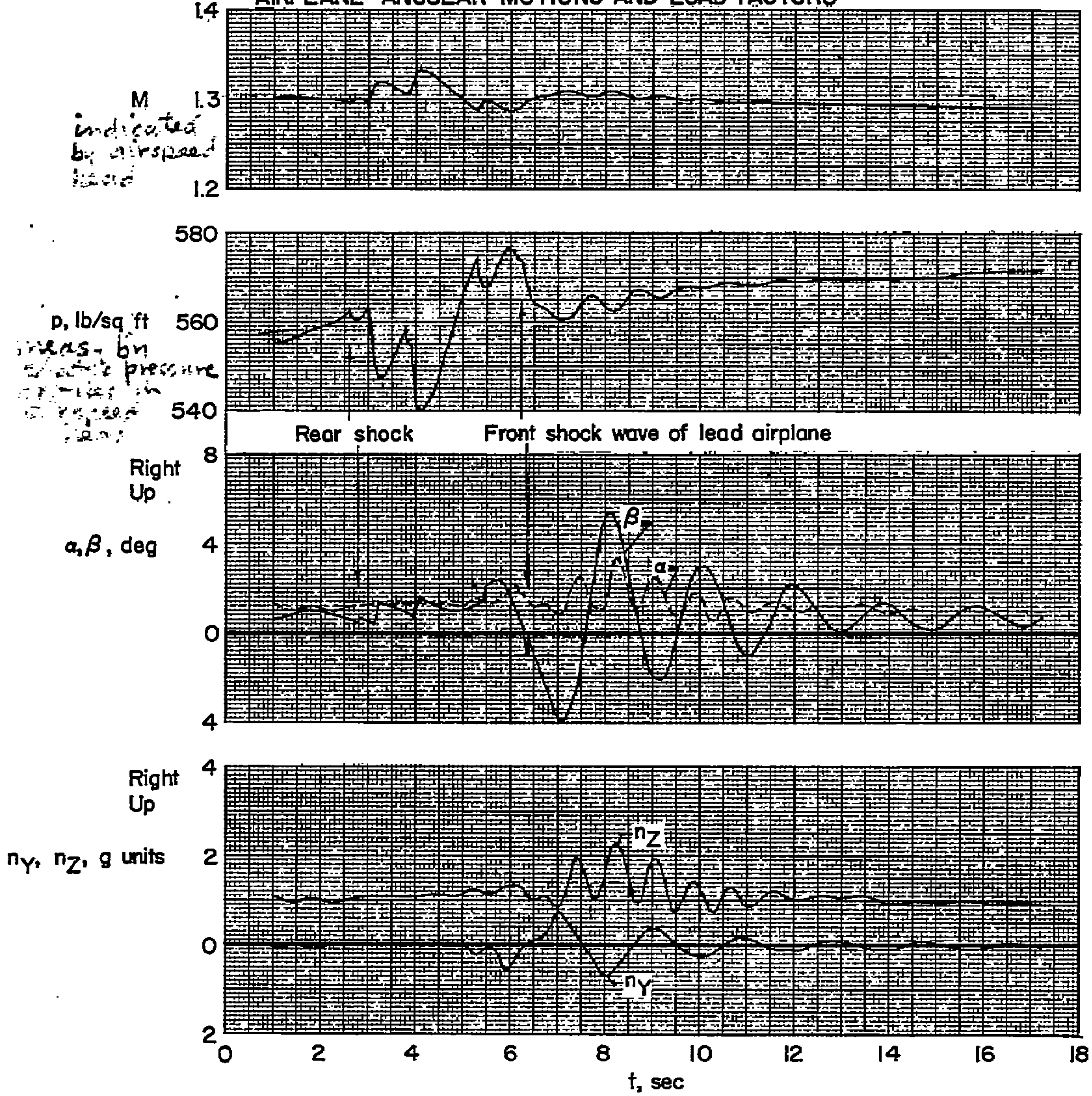

Figure 5(a)

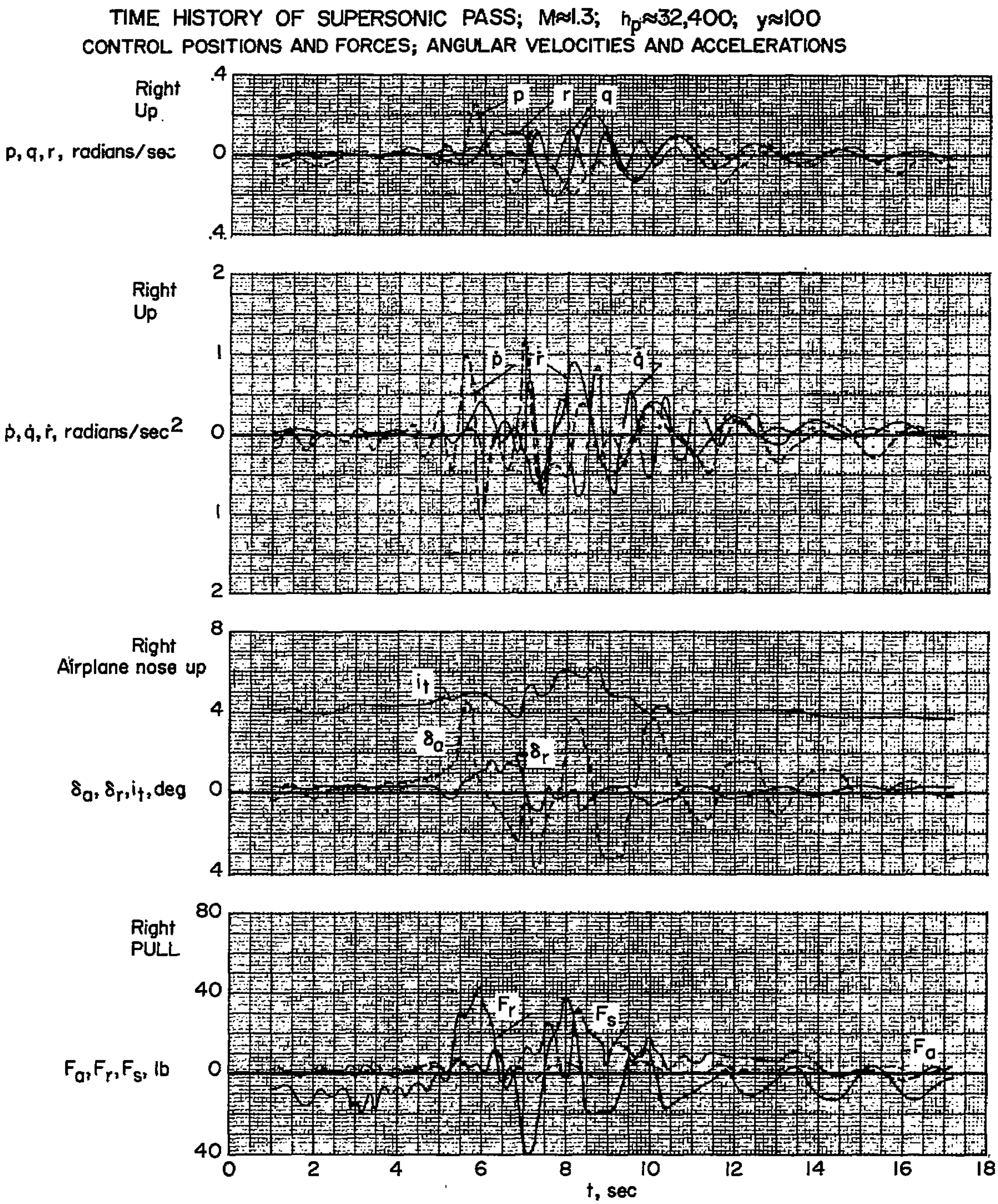
TIME HISTORY OF SUPERSONIC PASS; M≈1.3; h_p≈32,400; y≈100
CONTROL POSITIONS AND FORCES; ANGULAR VELOCITIES AND ACCELERATIONS
Right
Up
p, q, r, radians/sec
.4
0
.4
p
r
q
Right
Up
$\dot{p}, \dot{q}, \dot{r}$, radians/sec^2
2
1
0
1
2
$\dot{p}$
$\dot{r}$
$\dot{q}$
Right
Airplane nose up
δ_a, δ_r, i_t, deg
8
4
0
4
i_t
δ_a
δ_r
Right
PULL
F_a, F_r, F_s, lb
80
40
0
40
F_r
F_s
F_a
0
2
4
6
8
10
12
14
16
18
t, sec

Figure 5(b)

TIME HISTORY OF SUPERSONIC PASS; $M \approx 1.3$; $h_p \approx 32{,}400$; $y \approx 100$

VERTICAL-TAIL STRUCTURAL LOADS

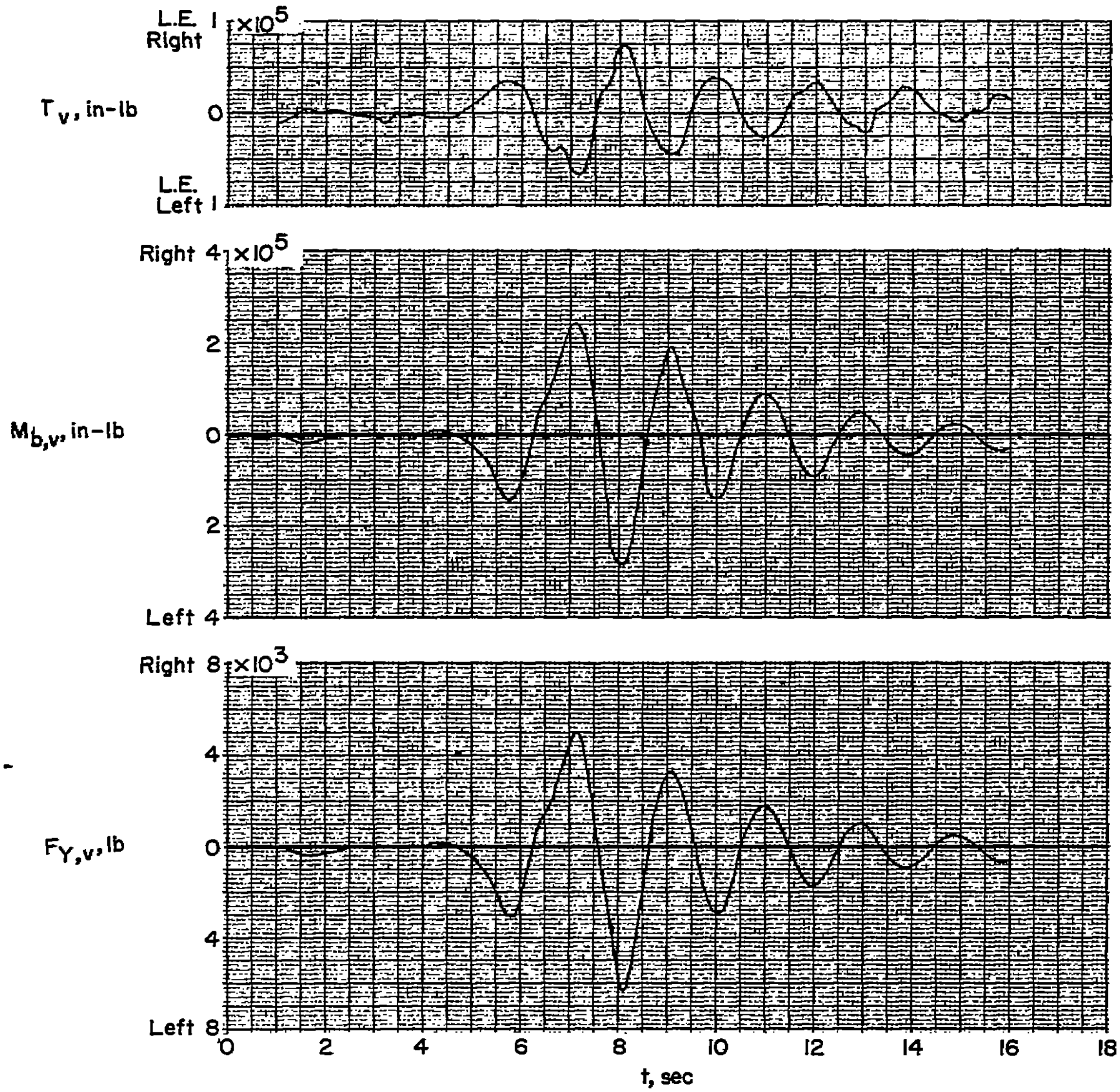

Figure 5 (c)

SUMMARY OF SUPERSONIC PASSES

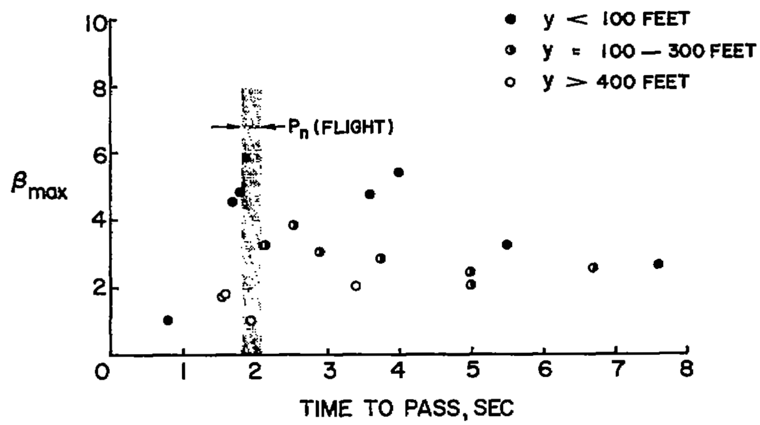

Figure 6

COMPARISON OF CALCULATED AND EXPERIMENTAL
MAXIMUM SIDESLIP ANGLES

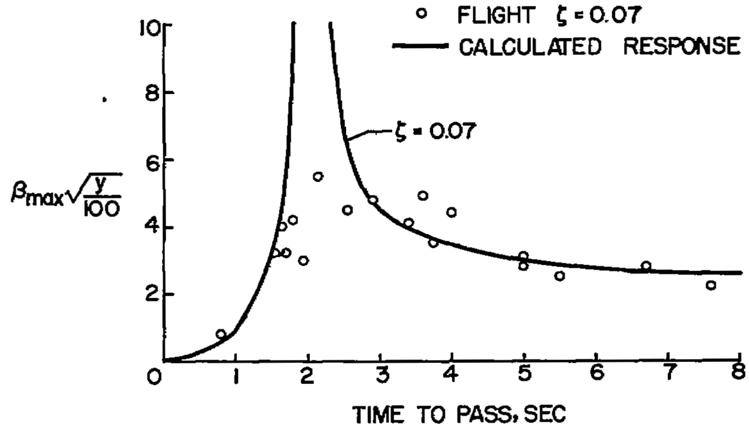

Figure 7

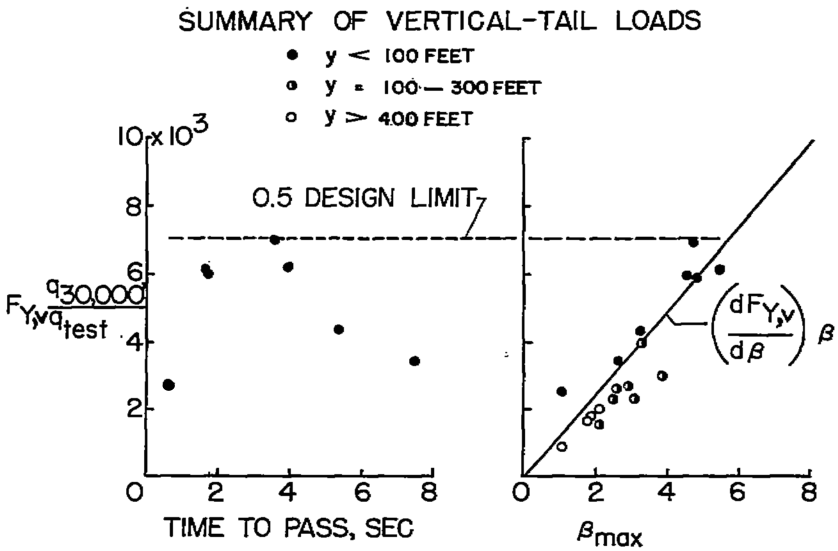
SUMMARY OF VERTICAL-TAIL LOADS
y < 100 FEET
y = 100 — 300 FEET
y > 400 FEET
10 x 10^3
8
6
4
2
0
0.5 DESIGN LIMIT
$F_{Y,v}\frac{q_{30,000}}{q_{test}}$
$\left(\frac{dF_{Y,v}}{d\beta}\right)\beta$
0 2 4 6 8
TIME TO PASS, SEC
0 2 4 6 8
β_{max}

Figure 8